ELSEVIER Journal of Computational and Applied Mathematics 69 (1996) 125–142

JOURNAL OF COMPUTATIONAL AND APPLIED MATHEMATICS

Pseudospectra for the wave equation with an absorbing boundary

Tobin A. Driscoll[a,*,1], Lloyd N. Trefethen[b,2]

[a] *Center for Applied Mathematics, Cornell University, Ithaca, NY 14853, United States*
[b] *Department of Computer Science, Cornell University, Ithaca, NY 14853, United States*

Received 13 May 1994; revised 23 January 1995

Abstract

For systems which can be described by $u_t = Au$, with a highly nonnormal matrix or operator A, the spectrum of A may describe the behavior of the system poorly. One such operator arises from the one-dimensional wave equation on a finite interval with a homogeneous Dirichlet condition at one end and a linear damping condition at the other. In this paper the pseudospectra (norm of the resolvent) of this operator are computed in an energy norm, using analytical techniques and computations with discrete approximations. When the damping condition is perfectly absorbing, the pseudospectra are half-planes parallel to the imaginary axis, and in other cases they are periodic in the imaginary direction and approximate strips of finite thickness. The nonnormality of the operator is related to the behavior of the system and the limitations of spectral analysis.

Keywords: Pseudospectra; Resolvent; Wave equation; Absorbing boundary condition

AMS classification: 35L05; 35B30; 35P99; 47A10

1. Introduction

Often in applied mathematics one obtains an initial value problem of the form $u_t = Au$, where each $u(t)$ is an element of a Hilbert space $\mathscr{H}$ and A is a linear operator defined on some or all of $\mathscr{H}$. Formally the solution is given by $u(t) = e^{tA}u(0)$, where e^{tA} is a suitably defined evolution operator, i.e., the semigroup generated by A. One way to analyze such a system is to determine $\Lambda(A)$, the spectrum of A. In particular, if the spectral abscissa $\sigma(A) = \sup\{\mathrm{Re}\,\lambda: \lambda \in \Lambda(A)\}$ is negative, $\|e^{tA}\|$ typically (but not always for infinite-dimensional $\mathscr{H}$ [1, 15, 25]) decays exponentially as $t \to \infty$.

However, spectral analysis may be incomplete. A difficulty arises when the eigenmodes of A are not orthogonal in $\mathscr{H}$—that is, the operator A is not *normal* (for simplicity, we assume the spectrum

* Corresponding author. E-mail: driscoll@cam.cornell.edu.

[1] This research was supported in part by a National Science Foundation Graduate Fellowship.
[2] Supported by NSF Grant DMS-9116110 and by D.E Grant DE-FG02-94ER25199.

SSDI 0377-0427(95)00021-6

consists entirely of eigenvalues corresponding to a complete set of eigenmodes). If the eigenmodes form an ill-conditioned basis, spectral analysis tends to miss short-term behavior patterns in the time evolution of the system, because a combination of such modes over a finite time interval need not grow or decay like its constituent parts.

Because sometimes we are concerned only with asymptotic behavior, we can sometimes ignore the effects of nonnormality. In other circumstances, however, a knowledge of the asymptotic behavior may not be as valuable as it at first seems. Such a situation has been recognized recently in the field of hydrodynamic stability [2, 4, 16, 22]. A perturbation to a laminar fluid flow may be asymptotically stable according to linear analysis, yet experience transient growth by factors of thousands. In some situations it appears to be this linear, nonmodal growth that triggers the transition to turbulence.

In this paper we present a simple, physically motivated case study of a situation in which nonnormality renders a spectral analysis incomplete. Our example is the one-dimensional wave equation with a Dirichlet condition at one end and a linear damping condition at the other; for related work, see [5, 10, 19, 23]. The physics is elementary enough to admit an exact description of the system's behavior, which is presented in Section 2. This behavior is compared with the results of spectral analysis in Section 3. In Section 4 we consider pseudospectra [21] and show that the degree of nonnormality is related to the limitations of the spectral analysis. Section 5 discusses the properties of various discretizations of the problem. Finally, Section 6 summarizes our results.

2. Behavior of the system

Consider the linear wave equation on $[0, \pi]$,

$$\phi_{tt}(x, t) - \phi_{xx}(x, t) = 0, \quad t \geqslant 0, \quad x \in [0, \pi], \tag{1}$$

subject to the boundary conditions

$$\phi(0, t) = 0, \tag{2}$$

$$\phi_x(\pi, t) + \delta\phi_t(\pi, t) = 0. \tag{3}$$

These equations model the vibration of an ideal string with left end pinned and right end subjected to damping with real parameter δ. This problem has been studied by Veselić as the continuous analog of a linearly arranged system of coupled oscillators with dashpot damping at one end [23]. More on this connection will be discussed in Section 5.

An investigation of the time evolution of solutions to (1)–(3) is straightforward. Disturbances propagate at unit speed without change except at reflections. Reflection at the left boundary $x = 0$ simply inverts the wave. The behavior at $x = \pi$ is more interesting; the reflection coefficient is easily seen to be

$$R_\pi = \frac{1 - \delta}{1 + \delta}. \tag{4}$$

In Fig. 1, R_π is plotted against δ. When $\delta = 1$, the damping becomes critical: R_π vanishes, and the energy is zero for $t \geqslant 2\pi$ for any initial condition. This parameter value corresponds to the zeroth-order absorbing boundary condition familiar in the numerical solution of PDEs [7].

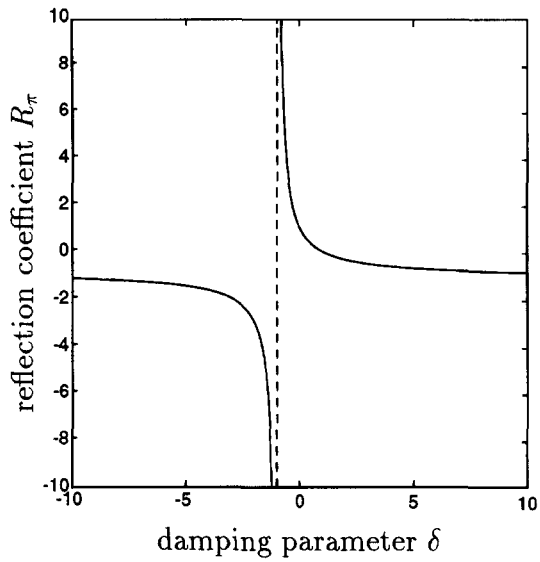

Fig. 1. Dependence of the reflection coefficient on the damping parameter δ.

Note that changing the sign of δ changes R_π to its reciprocal. This is a consequence of a time symmetry in (1)–(3), for replacing δ by $-\delta$ in these equations is equivalent to replacing t by $-t$. Thus, positive values of δ cause physical damping while negative values actually input energy. Another symmetry is that replacing δ by $1/\delta$ simply changes the sign of R_π, i.e., the parity of the reflection. Because of these symmetries, we henceforth restrict attention to $\delta \in [0, 1]$.

For any suitably localized initial condition, the amplitude of the solution changes by a factor of R_π near each time $t + 2n\pi$, where $n \in \mathbb{Z}$, and $0 < t < 2\pi$. The degree of localization in space of the initial disturbance is proportional to the localization in time of its change in amplitude. By choosing an initial condition with all its energy near $x = \pi$, we can make the transitions arbitrarily sharp and make t arbitrarily close to 2π. This description of the system's behavior will be stated more formally in the next section.

3. Spectral analysis

We now discuss two ways to reformulate (1)–(3) as a first-order linear evolution process on a Hilbert space. We then compare the information obtained from the spectrum of the resulting operator with the system's behavior.

To begin, we let

$$u = \begin{bmatrix} u_1 \\ u_2 \end{bmatrix} = \begin{bmatrix} \phi_x \\ \phi_t \end{bmatrix}. \tag{5}$$

Then

$$u_t = Lu, \quad L := \begin{bmatrix} 0 & \mathrm{d}/\mathrm{d}x \\ \mathrm{d}/\mathrm{d}x & 0 \end{bmatrix}, \tag{6}$$

where the domain $D(L)$ of L is the dense [9] subspace of $\mathscr{H} = L^2[0, \pi] \times L^2[0, \pi]$ consisting of pairs of absolutely continuous functions with derivatives in $L^2[0, \pi]$ and which satisfy the boundary conditions

$$u_2(0) = 0, \tag{7}$$

$$u_1(\pi) + \delta u_2(\pi) = 0. \tag{8}$$

The form (6) is sometimes called the symmetric hyperbolic form [8], and is a natural way to pose the problem in the sense that the squared norm on $\mathscr{H}$ is the energy of the string:

$$\|u\|^2 = \int_0^\pi \|u(x)\|_2^2 \, \mathrm{d}x = \int_0^\pi (|\phi_x(x)|^2 + |\phi_t(x)|^2) \, \mathrm{d}x. \tag{9}$$

The second reformulation involves unwrapping (6)–(8) to obtain a first-order problem involving just one independent variable, but on a periodic domain of length 2π rather than π. We first define the characteristic variables

$$v = \frac{1}{\sqrt{2}} \begin{bmatrix} 1 & 1 \\ 1 & -1 \end{bmatrix} u. \tag{10}$$

The boundary conditions become

$$v_1(0) = v_2(0), \tag{11}$$

$$v_1(\pi) = -R_\pi v_2(\pi). \tag{12}$$

Now we define the scalar function $w \in L^2[-\pi, \pi]$ by

$$w(x) = \begin{cases} v_2(-x), & -\pi \leqslant x \leqslant 0, \\ v_1(x), & 0 \leqslant x \leqslant \pi. \end{cases} \tag{13}$$

Condition (11) ensures that w is differentiable with respect to t and x at $x = 0$, and it is easily verified that

$$w_t = \tilde{L} w, \quad \tilde{L} := \mathrm{d}/\mathrm{d}x. \tag{14}$$

Condition (11) is now implicit and (12) becomes

$$w(\pi) = -R_\pi w(-\pi); \tag{15}$$

that is, the domain is periodic and waves which reach $x = -\pi$ are wrapped back to $x = \pi$. It is easily checked that

$$\|w\|^2 = \int_{-\pi}^{\pi} |w(x)|^2 \, \mathrm{d}x = \|u\|^2, \tag{16}$$

and so the two formulations are unitarily similar. In particular, this means that the spectrum and norm of the resolvent are the same for L and $\tilde{L}$. For the most part, in what follows we use the form

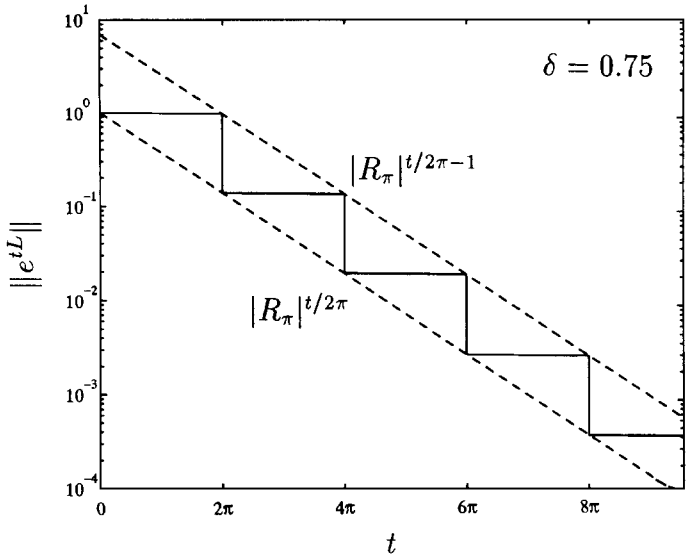

Fig. 2. Exact solution operator norm (solid) and eigenvalue envelopes (dashed) for $\delta = 0.75$. The lower envelope is given by (20) and the upper envelope is a constant multiple of the lower one, given by Eq. (26) in Section 4. Here the damping parameter is $\delta = 0.75$; with $\delta = 1$, the norm drops to 0 at $t = 2\pi$.

(6)–(8), because it does not exploit the special form of the boundary conditions and thus is more readily generalized.

The discussion of the last section implies that the solution operator for (6), e^{tL}, satisfies

$$\|e^{tL}\| = |R_\pi|^{\lfloor t/2\pi \rfloor}, \tag{17}$$

where $\lfloor \cdot \rfloor$ is the floor (truncation to integer) function.[3] Fig. 2 displays this stairstep evolution. For $\delta = 1$ the norm is one for $t < 2\pi$ and zero thereafter.

The spectrum of L is easily determined. From (6) and (7) we see that if u is an eigenfunction it must have the form

$$u_\lambda = \begin{bmatrix} \cosh \lambda x \\ \sinh \lambda x \end{bmatrix} \tag{18}$$

for values of λ to be determined by the remaining boundary condition. From (8) we conclude that for $\delta = 1$, the spectrum is empty, and for $\delta \neq 1$ the spectrum is the set of eigenvalues[4]

$$\lambda_n = \frac{1}{2\pi} \log\left(\frac{1-\delta}{1+\delta}\right) + \left(n + \frac{1}{2}\right) \mathrm{i} \tag{19}$$

[3] Notwithstanding that L is unbounded and defined only a proper subspace of $\mathscr{H}$, the solution operator $\exp(tL)$ is a bounded operator on all of $\mathscr{H}$ for any $t \geqslant 0$ and $\delta \geqslant 0$. This is a standard situation in the theory of semigroups; see [14]. We use the suggestive exponential notation even though the semigroup cannot be defined simply by a power series.

[4] In the next section we derive a bound for the norm of the resolvent which verifies that the point spectrum derived here is the entire spectrum.

for all $n \in \mathbb{Z}$. The spectrum is plotted in Figs. 3 and 4 for two values of δ. The fact that infinitely many eigenvalues have the same real part allows the steps in Fig. 2 to repeat indefinitely. Otherwise, the solution would eventually be dominated by finitely many eigenmodes and $\|e^{tL}\|$ would necessarily smooth out as $t \to \infty$.

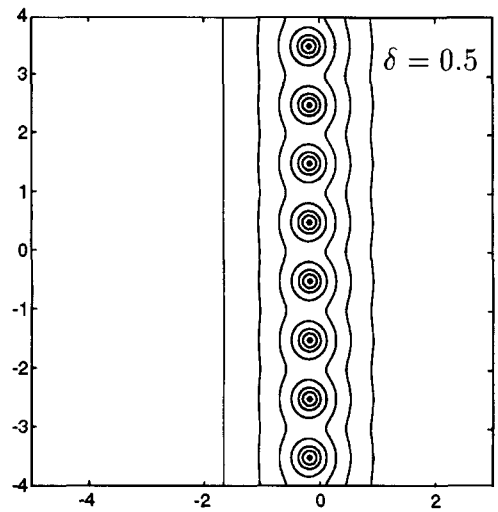

Fig. 3. Boundaries of ε-pseudospectra of L for $\delta = 0.5$. Values of ε are (inner to outer) $10^{-1}, 10^{-0.8}, \ldots, 10^{0}$. The pseudospectra are inside the boundaries. The spectrum is marked by dots.

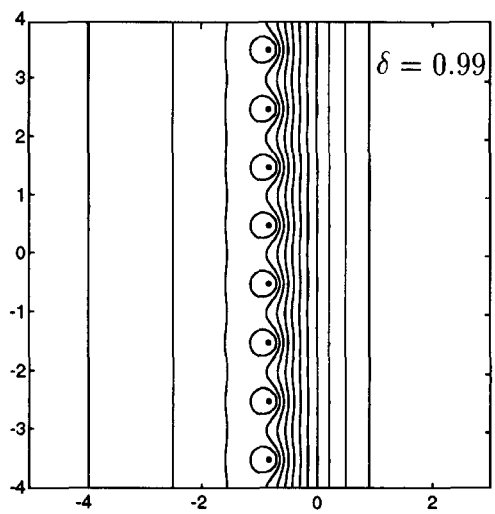

Fig. 4. Boundaries of $\Lambda_\varepsilon(L)$ for $\delta = 0.99$. Values of ε are (inner to outer) $10^{-2}, 10^{-1.8}, \ldots, 10^{0}$. The left boundaries of the last seven are not visible on this scale.

In one respect the spectrum of L corresponds exactly to the behavior of e^{tL}. Observe that

$$|e^{\lambda_n t}| = \exp\left(\frac{t}{2\pi}\log\frac{\delta-1}{\delta+1}\right) = |R_\pi|^{t/2\pi}, \tag{20}$$

which is clearly related to (17). In Fig. 2 we see that (20) is a smooth lower bound for $\|e^{tL}\|$, having identical asymptotic behavior. Put simply, the spectral abscissa of L coincides with the *exponential type* of e^{tL}:

$$\sigma(L) = \lim_{t\to\infty} t^{-1}\log\|e^{tL}\|. \tag{21}$$

Note that both sides of (21) are $-\infty$ when $\delta = 1$.

Fig. 2 also makes it obvious that there is more to $\|e^{tL}\|$ than is described by (20). The step behavior results from transient deviations from the asymptotic trend. As we shall see in the next section, these transient behaviors are due to the nonnormality of L.

4. Pseudospectral analysis

Let A be a closed linear operator on a Banach space X with norm $\|\cdot\|$, and let $\Lambda(A)$ and $\rho(A)$ denote the spectrum and resolvent set of A, respectively. For any $\varepsilon > 0$, we define the *ε-pseudospectrum* of A by

$$\Lambda_\varepsilon(A) = \{\lambda \in \rho(A): \|(\lambda I - A)^{-1}\| \geq \varepsilon^{-1}\} \cup \Lambda(A), \tag{22}$$

and we set $\Lambda_0(A) = \Lambda(A)$. Intuitively, the resolvent norm is infinite in the spectrum, and large in an ε-pseudospectrum for small ε. Another characterization is

$$\Lambda_\varepsilon(A) = \text{closure}\{\lambda \in \mathbb{C}: \lambda \in \Lambda(A+E) \text{ for some } \|E\| \leqslant \varepsilon\}. \tag{23}$$

It is well known that if A is normal, then $\Lambda_\varepsilon(A)$ is the union of ε-balls around all points in $\Lambda(A)$ (see [9, p. 277]). The degree to which the pseudospectra are larger than this is a measure of the nonnormality of A.

Fig. 3–5 show the boundaries of several pseudospectra of L for three values of δ. The computations which produced these figures are discussed in Section 5. Note that when δ is not near 1, the degree of nonnormality is mild. Recall that $|R_\pi| \to 1$ as $\delta \to 0$, and the smooth spectral approximation in (20) becomes increasingly good. In fact, by finding the adjoint of L we see that L is normal in this limit. On the other hand, for $\delta \approx 1$, the reflection coefficient is approximately 0 and the spectral approximation is not so good. Fig. 4 confirms that L is further from normal in this situation, especially in the left half-plane. With $\delta = 1$, the norm of the solution to (6) drops to zero in a finite time, and the spectrum is empty. Fig. 5 shows that the operator is highly nonnormal in this case, much more so than for even nearby δ. (Note the different contour levels in this figure.)

One way to quantify the degree of nonnormality for this family of operators is to compute the condition number of a basis of eigenfunctions. To do this it suffices to find the condition number of a transformation $M: \mathscr{H} \to \mathscr{H}$ that maps the eigenfunctions (18) onto an orthogonal basis. Since L is normal when $\delta = 0$, the eigenfunctions in this case provide a natural choice for the orthogonal

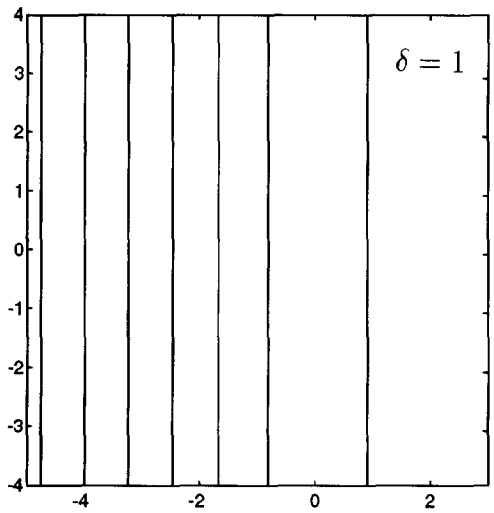

Fig. 5. Boundaries of $\Lambda_\varepsilon(L)$ for $\delta = 1$. Values of ε are (left to right) $10^{-12}, 10^{-10}, \ldots, 10^{0}$. The pseudospectra are the half-planes to the left of these boundaries.

basis. The mapping is then

$$Mu = \begin{bmatrix} \cosh \alpha x & \sinh \alpha x \\ \sinh \alpha x & \cosh \alpha x \end{bmatrix} u, \tag{24}$$

where $\alpha = \operatorname{Re} \lambda_n = \log(|R_\pi|)/2\pi$. It is straightforward to show that

$$\kappa(M) = \sup_{x \in [0,\pi]} \kappa_2 \left(\begin{bmatrix} \cosh \alpha x & \sinh \alpha x \\ \sinh \alpha x & \cosh \alpha x \end{bmatrix} \right) = \frac{1}{R_\pi}, \tag{25}$$

where R_π is the reflection coefficient given by (4). This is a particularly clean expression of the degree of nonnormality of L as δ ranges from 0 to 1 (R_π ranges from 1 to 0). We can now explain the upper envelope for the solution norm plotted in Fig. 2; it is

$$\kappa(M)|e^{\lambda_n t}| = |R_\pi|^{t/2\pi - 1}. \tag{26}$$

A more detailed quantification of the nonnormality is the relative size of each ε-pseudospectrum, which we define as

$$\nu(\delta, \varepsilon) = \frac{\text{Re-diameter of } \Lambda_\varepsilon(L)}{2\varepsilon}. \tag{27}$$

Here "Re-diameter" means the extent of the pseudospectrum in the real direction of the complex plane. Clearly, $\nu(0, \varepsilon) = 1$ and $\nu(1, \varepsilon) = \infty$ for all ε, corresponding to the normal and strongly nonnormal cases, respectively. Fig. 6 shows ν for various values of δ and ε. In the limit $\varepsilon \to 0$, $\nu(\delta, \varepsilon)$

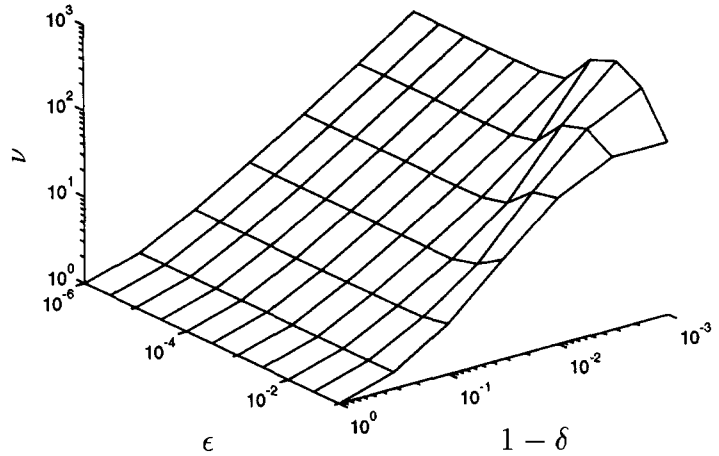

Fig. 6. One way to measure nonnormality, see text.

becomes the condition number of the eigenvalues,[5] which can be computed exactly as

$$v(\delta, 0) = \frac{|R_\pi| - 1/|R_\pi|}{2\log|R_\pi|}. \tag{28}$$

When $|R_\pi|^{-1}$ is large, (25) is larger than (28) by a factor which is asymptotically $-2\log|R_\pi|$, suggesting an interaction between eigenvalues. Correspondingly, as ε increases, v undergoes a temporary increase (the ripple in the surface of Fig. 6), indicating that the pseudospectra reflect some coupling across individual eigenvalues.

Some of the features evident in Figs. 3–5 can be derived analytically. The following theorem summarizes this information.

Theorem 1. *For $0 < \delta \leqslant 1$, the numerical range of L is the closed left half-plane, and for $\delta = 0$ it is the imaginary axis. Consequently,*

$$\|(\lambda I - L)^{-1}\| \leqslant (\operatorname{Re}\lambda)^{-1}, \quad \operatorname{Re}\lambda > 0. \tag{29}$$

For $0 < \delta < 1$ the spectrum of L is given by (19). *The resolvent norm is invariant under translations by* $i\mathbb{Z}$ *and satisfies*

$$\|(\lambda I - L)^{-1}\| \geqslant \left|1 - \frac{1}{2R_\pi}\right| \cdot |\operatorname{Re}\lambda|^{-1} + O(e^{2\pi \operatorname{Re}\lambda}), \quad \operatorname{Re}\lambda \to -\infty, \tag{30}$$

$$\|(\lambda I - L)^{-1}\| \leqslant \left(1 + \frac{1}{2R_\pi}\right) \cdot |\operatorname{Re}\lambda|^{-1} + O(e^{2\pi \operatorname{Re}\lambda}), \quad \operatorname{Re}\lambda \to -\infty. \tag{31}$$

[5] If $\lambda \in \Lambda(A)$ and u and v are unit elements such that $Au = \lambda u$ and $A^*v = \bar{\lambda}v$, the condition number of λ is $\kappa(\lambda) = 1/(u, v)$.

For $\delta = 1$ the spectrum of L is empty. The resolvent norm is invariant under all imaginary translations and satisfies

$$\|(\lambda I - L)^{-1}\| = \frac{e^{2\pi|\mathrm{Re}\,\lambda|}}{2|\mathrm{Re}\,\lambda|} + O(|\mathrm{Re}\,\lambda|^{-1}), \quad \mathrm{Re}\,\lambda \to -\infty. \tag{32}$$

Proof. To determine the numerical range, we compute

$$(u, Lu) = \int_0^\pi (\overline{u_2'} u_1 + \overline{u_1'} u_2)\,dx \tag{33}$$

$$= [\overline{u_2} u_1]_0^\pi + \int_0^\pi (-\overline{u_2} u_1' + \overline{u_1'} u_2)\,dx \tag{34}$$

$$= -\delta |u_2(\pi)|^2 + \int_0^\pi (\overline{u_1'} u_2 - \overline{u_2} u_1')\,dx, \tag{35}$$

where the last line is due to (7)–(8). Note that the integrand is imaginary. Restriction to $\|u\| = 1$ clearly does not limit the choice of $u_2(\pi)$, and because of the derivative of u_1 in the integrand, any imaginary value can be achieved. Thus, the assertions about the numerical range are proved. Inequality (29) is a standard consequence [14, p. 12]. Note that for any value of δ, the numerical abscissa, or maximum real part of the numerical range, is zero. This explains the slope of the steps in Fig. 2.

Now we establish the translation invariances. Let S_β be the family of unitary operators on $\mathscr{H}$ defined by

$$S_\beta u = \begin{bmatrix} \cos\beta x & i\sin\beta x \\ i\sin\beta x & \cos\beta x \end{bmatrix} u. \tag{36}$$

This operator is motivated by the eigenfunctions (18), because $S_\beta u_\lambda = u_{\lambda + i\beta}$. In general, $S_\beta u$ will not satisfy the boundary conditions (7) and (8) even when $u \in D(L)$, but they are satisfied whenever $\beta = n \in \mathbb{Z}$. Moreover,

$$\|((\lambda + in)I - L) S_n u\| = \|(\lambda I - L)u\|. \tag{37}$$

From this it is easily seen that the resolvent norm, and hence the pseudospectra, are invariant under translations of $i\mathbb{Z}$, just as are the spectra from (19).

The conclusion is stronger in the critically damped case. When $\delta = 1$, S_β maps $D(L)$ into $D(L)$ for any value of $\beta \in \mathbb{R}$. Hence, the pseudospectra of L are invariant under all purely imaginary translations.

For the expressions (30)–(32) in the left half-plane we parallel the development in [18]. It is convenient here to use $\tilde{L}$, given by (14) and (15), which is unitarily similar to L.

First we decompose $(\lambda I - \tilde{L})^{-1}$ into two parts:

$$(\lambda I - \tilde{L})^{-1} = R_1 + R_2, \tag{38}$$

where R_1 is given explicitly by

$$(R_1 f)(x) = \int_{-\pi}^x e^{\lambda(x-y)} f(y)\,dy. \tag{39}$$

The operator R_1 solves $(\lambda I - \tilde{L})w = f$ without the boundary condition (15), and (39) results from the Green's function for this problem. Now $R_1 f$ is the restriction to $[-\pi, \pi]$ of the convolution $f * g$, where f is extended by zero to $(-\infty, \infty)$, and $g(s) = e^{\lambda s}$ for $s > 0$ and is zero for $s < 0$. By Fourier transformation,

$$\begin{aligned} \|R_1\| &\leqslant \sup_{\xi \in \mathbb{R}} |\hat{g}(\xi)| \\ &= \sup_{\xi \in \mathbb{R}} |(i\xi - \lambda)^{-1}| \\ &= |\operatorname{Re} \lambda|^{-1}. \end{aligned} \tag{40}$$

The role of R_2 is to make the result of (38) satisfy the boundary condition (15). Since $(\lambda I - \tilde{L})$ annihilates $e^{\lambda x}$, we let

$$(R_2 f) = a e^{\lambda x} \tag{41}$$

for a constant a. From (15), (38), and (39) we see that

$$\begin{aligned} a &= (e^{\lambda\pi} - R_\pi e^{-\lambda\pi})^{-1} (R_\pi (R_1 f)(-\pi) - (R_1 f)(\pi)) \\ &= -(1 - R_\pi e^{-2\lambda\pi})^{-1} \int_{-\pi}^{\pi} e^{-\lambda s} f(s)\, ds. \end{aligned} \tag{42}$$

To bound the integral in (42) we use the Cauchy–Schwarz inequality, and in choosing f we may make this bound sharp. Then from (41) and (42) we find

$$\|R_2\| = \left| \frac{e^{2\pi \operatorname{Re}\lambda} - e^{-2\pi \operatorname{Re}\lambda}}{2 \operatorname{Re}\lambda (1 - R_\pi e^{-2\pi\lambda})} \right|. \tag{43}$$

Finally, (30)–(32) follow from the inequalities

$$|\|R_1\| - \|R_2\|| \leqslant \|R_1 + R_2\| \leqslant \|R_1\| + \|R_2\|. \quad \square$$

For δ far from 1, inequalities (29) and (31) confirm the relatively mild degree of nonnormality observed in Fig. 3. For $\delta \approx 1$, the lower bound (30) guarantees that the pseudospectra penetrate much farther into the left half-plane, as can be seen in Fig. 4; however, each pseudospectrum is still bounded on the left and right. For $\delta = 1$ the estimate (32) in the left half-plane explains the unboundedness of the pseudospectra as $\operatorname{Re}\lambda \to -\infty$ and the spacing of the contours in Fig. 5. Moreover, it follows that L must be nilpotent in the sense that $e^{tL} = 0$ for $t \geqslant 2\pi$. In fact, we have the following general theorem relating nilpotency of the solution operator to the growth of the resolvent norm at infinity.

Theorem 2. *Suppose A is a linear operator which generates the C_0 semigroup*[6] e^{tA} *on the Hilbert space H. Then $e^{tA} = 0$ for all $t \geqslant t_0$ if and only if the spectrum of A is empty and $\|(\lambda I - A)^{-1}\| = O(e^{-t_0 \operatorname{Re}\lambda})$ as $\operatorname{Re}\lambda \to -\infty$.*

[6] The term C_0 *semigroup* means that for each $x \in H$, $e^{tA}x$ is continuous in H as a function of t. By the Hille–Yosida–Phillips theorem, this is equivalent to A being closed, $D(A)$ being dense in H, and a generalization of the bound (29); see [14].

Proof. We prove this theorem with an application of the Paley–Wiener theorem for Fourier transforms of functions with compact support [6]. We start with the Laplace transform

$$(\lambda I - A)^{-1}x = \int_0^\infty e^{-t\lambda}e^{tA}x\,dt, \tag{44}$$

valid for all $x \in H$ (see [14, p. 20]). Since e^{tA} is C_0, there exist real M and ω such that $\|e^{tA}\| \leqslant Me^{t\omega}$ for all $t \geqslant 0$ (by the uniform boundedness principle; see [14, p. 4]). Choose $\gamma > \omega$ and fix x and y in H with $\|x\| = \|y\| = 1$. Now by (44),

$$\begin{aligned}([(\gamma + \lambda)I - A]^{-1}x, y) &= \left(\int_0^\infty e^{-t\lambda}e^{-t\gamma}e^{tA}x\,dt, y\right)\\ &= \int_0^\infty e^{-t\lambda}(e^{-t\gamma}e^{tA}x, y)\,dt\\ &=: \int_{-\infty}^\infty e^{-t\lambda}f(t)\,dt,\end{aligned}$$

where the scalar function $f(t)$ is in L^2. The equivalence of the first two integrals is easily seen because $e^{tA}x$ is continuous in H as a function of t. We now recognize $F(\xi) := ([(\gamma + i\xi)I - A]^{-1}x, y)$ as the Fourier transform of f, and the Paley–Wiener theorem asserts that $f(t) = 0$ for all $t > t_0$ if and only if F is entire and $|F(\xi)| \leqslant Ce^{|\xi|t_0}$. By a Phragmén–Lindelöf theorem, this latter bound is equivalent to

$$|F(\xi)| \leqslant Ce^{t_0 \operatorname{Im}\xi}, \quad \operatorname{Im}\xi > 0,$$

which in turn is equivalent to

$$|((\lambda I - A)^{-1}x, y)| \leqslant Ce^{-t_0(\operatorname{Re}\lambda - \gamma)}, \quad \operatorname{Re}\lambda < \gamma.$$

The conclusion $f(t) = 0$ for $t > t_0$ can be extended to $t = t_0$ by the C_0 property. Since x and y are arbitrary unit elements, the proof is complete. □

5. Discretizations

The bounds derived in Theorem 1 are not sharp enough to produce the plots of Figs. 3–5. These plots were made by discretizing the operator L to obtain a matrix A whose pseudospectra can be computed numerically via the singular value decomposition. It is presumed, on the basis of numerical evidence, that as the number of points in the discretization is increased, the pseudospectra of the matrix converge to those of the operator in the sense of (nonuniform) convergence of $\|(\lambda I - A)^{-1}\|$ for each $\lambda \in \rho(L)$.

One physically appealing discretization of a continuous string is the so-called loaded string [11], in which the mass is divided into equal lumps of mass m spaced evenly at a distance h apart. Suppose that the tension in the string is τ and that the vertical displacements u_i, $i = 0, \ldots, N$, of the masses are small. Then Newton's law in the interior of the string is

$$m\ddot{u}_i = \frac{\tau}{h}(u_{i-1} - 2u_i + u_{i+1}), \tag{45}$$

where $i = 2, \ldots, N-1$. If the mass density $\rho = m/h$ is fixed as $h \to 0$, then

$$\rho \ddot{u}_i = \tau \left(\frac{u_{i+1} - 2u_i + u_{i-1}}{h^2} \right). \tag{46}$$

Since the right-hand side of (46) is just a second-order finite difference, in the limit $h \to 0$ we recover the wave equation. The normalization in (1) requires that $\rho = \tau$.

We still have boundary conditions to consider. At the left end of the chain we require $u_0 = 0$, which corresponds to (7). At the right end we assume the existence of a linear dashpot that provides a damping force of size $\gamma \dot{u}_N$. Then

$$m\ddot{u}_N = \rho h \ddot{u}_N = -\tau \left(\frac{u_N - u_{N-1}}{h} \right) - \gamma \dot{u}_N, \tag{47}$$

which becomes

$$\tau (u_N)_x + \gamma (u_N)_t = 0 \tag{48}$$

in the limit $h \to 0$. Comparing this to (8), we recognize that $\delta = \gamma/\tau$.

Now suppose that instead of tension in the string supplying the forces between vertically displaced masses, the masses are connected to one another by springs of force constant κ and move horizontally (along the length of the chain). It is easy to see that the resulting equations are equivalent to (46) and (47) provided that $\kappa = \tau/h$. In matrix form they are

$$m\ddot{u} + \gamma C \dot{u} + \kappa K u = 0, \tag{49}$$

where $u = [u_1 \cdots u_N]^{\mathrm{T}}$ and

$$C = \operatorname{diag}(0, 0, \ldots, 0, 1), \quad K = \begin{bmatrix} 2 & -1 & & & \\ -1 & 2 & -1 & & \\ & \ddots & \ddots & \ddots & \\ & & \ddots & 2 & -1 \\ & & & -1 & 1 \end{bmatrix}. \tag{50}$$

We now follow Veselić [23] and define variables which transform (49) into a first-order system. Let $K = PP^{\mathrm{T}}$ be a Cholesky factorization and set

$$v = \begin{bmatrix} \sqrt{\kappa} P^{\mathrm{T}} & 0 \\ 0 & \sqrt{m} I \end{bmatrix} \begin{bmatrix} u \\ \dot{u} \end{bmatrix}. \tag{51}$$

As before, the variables have been chosen so that $\|v\|_2^2$ is the total energy of the system. Now

$$\dot{v} = \begin{bmatrix} 0 & \sqrt{\frac{\kappa}{m}} P^{\mathrm{T}} \\ -\sqrt{\frac{\kappa}{m}} P & -\frac{\gamma}{m} C \end{bmatrix} v = A_N v. \tag{52}$$

Using the relationships among the parameters we have

$$A_N = \frac{N}{\pi}\begin{bmatrix} 0 & P^{\mathrm{T}} \\ -P & -\delta C \end{bmatrix}. \tag{53}$$

We call the $2N \times 2N$ matrix A_N the order N loaded-string discretization of the continuous operator L. In light of (46) and (47), it is perhaps not surprising that A_N is also the matrix that results by taking appropriate finite-difference approximations to the differentials in (6) and imposing the boundary conditions (7) and (8) by row and column manipulations.

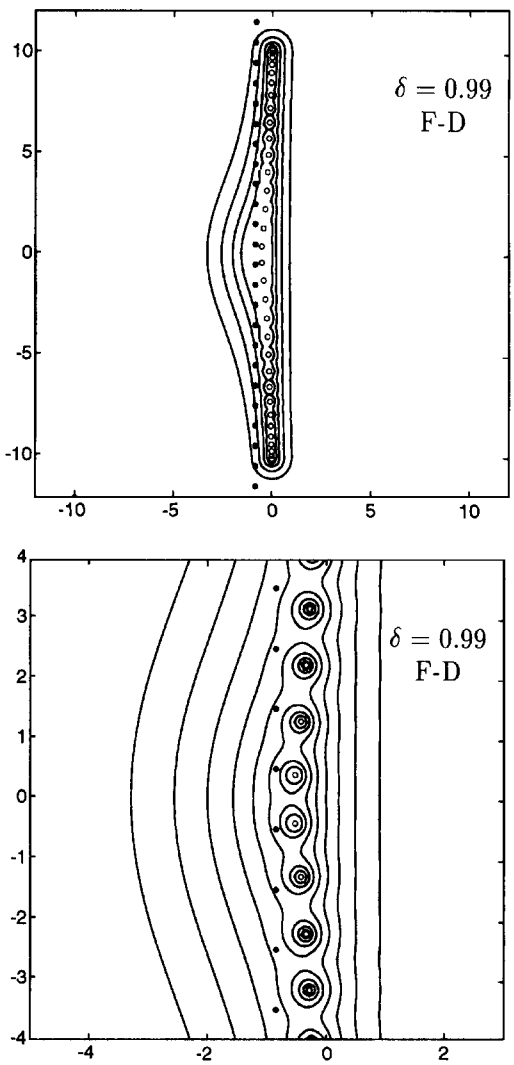

Fig. 7. Pseudospectra $\Lambda_\varepsilon(A_N)$ of the loaded-string discretization (53) with $N = 16$ and $\delta = 0.99$. Values of ε are (inner to outer) $10^{-0.6}, 10^{-0.4}, 10^{-0.2}, 10^{0}$ on the top, and additionally $10^{-0.8}, \ldots, 10^{-1.4}$ in the detail on the bottom (cf. Fig. 4). The eigenvalues of L are marked by dots and those of A_N are marked by circles.

Unfortunately, the spectra and pseudospectra of A_N converge to those of L rather slowly as $N \to \infty$. Fig. 7 shows the pseudospectra of A_N for $\delta = 0.99$, near the critical value, with $N = 16$. The agreement with Fig. 4 is unimpressive. Moreover, the results are virtually identical for $\delta = 1$, in contrast to the behavior for the exact operator L.

To improve the accuracy one might try more general mass, damping, and stiffness matrices in (49). Veselić, for example, has shown [24] that these matrices can be constructed to yield any predetermined set of eigenvalues. Instead, we choose to work directly from (6)–(8) using Chebyshev differentiation matrices for the derivatives in place of finite differences. A similarity transformation

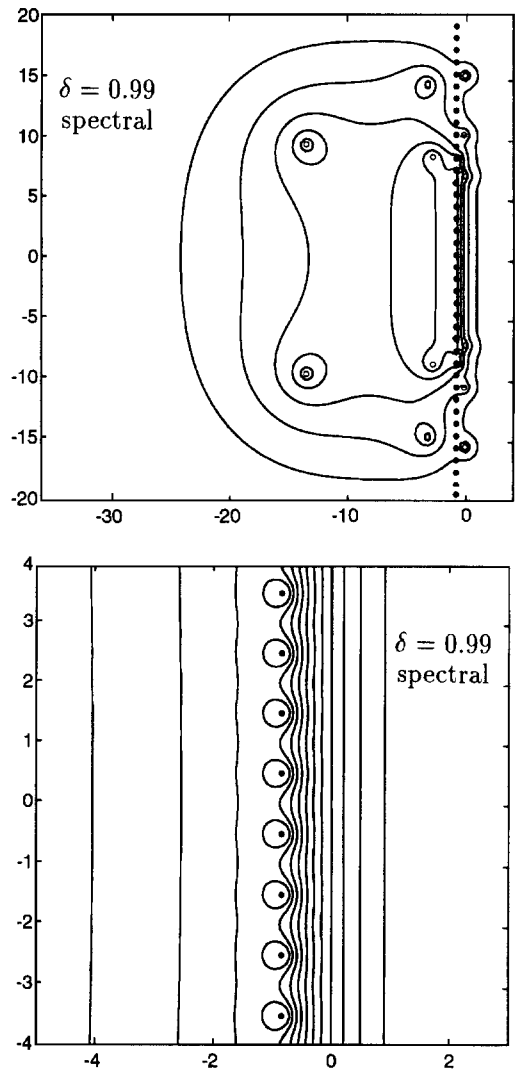

Fig. 8. Pseudospectra $\Lambda_\varepsilon(A_N)$ of the Chebyshev spectral discretization with $N = 16$ and $\delta = 0.99$. Values of ε are $10^{-1.6}, 10^{-1.2}, \ldots, 10^{0}$ on the top and the same as those of Fig. 4 in the detail on the bottom. There are two outlying eigenvalues of A_N not shown.

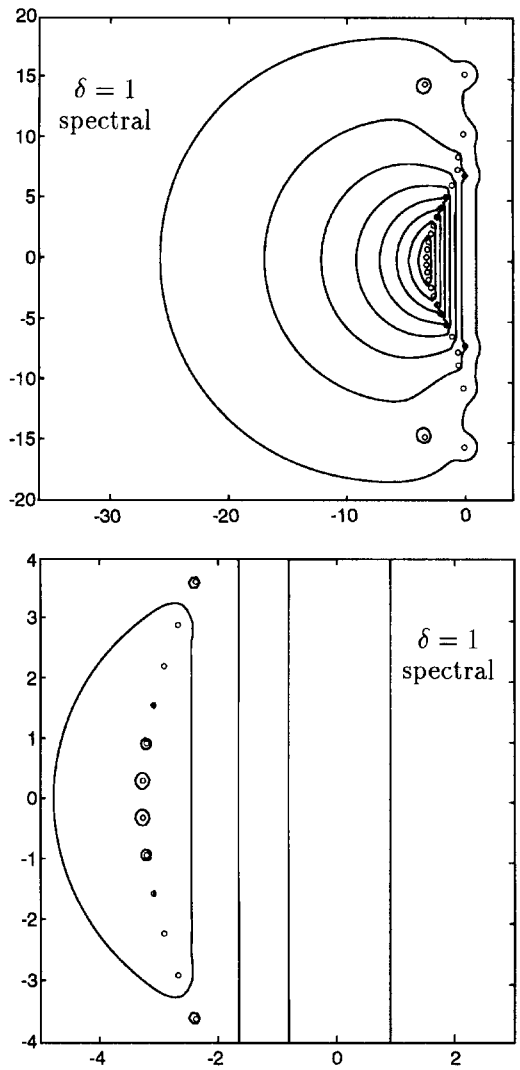

Fig. 9. Pseudospectra $\Lambda_\varepsilon(A_N)$ of the Chebyshev spectral discretization with $N = 16$ and $\delta = 1$. Values of ε are $10^{-7}, 10^{-6}, \ldots, 10^{0}$ on the top and $10^{-8}, 10^{-6}, \ldots, 10^{0}$ in the detail on the bottom (cf. Fig. 5). There are two outlying eigenvalues of A_N not shown.

using a weight matrix is needed so that the 2-norm of the result is the correct approximation to (9); see [16] for details. Figs. 8 and 9 show the results for $N = 16$. The agreement is far better than for the loaded string. Note that the $\delta = 1$ case is now qualitatively different, as required, and the properly spaced half-planes are well approximated.[7]

[7] See [18] for another comparison of the pseudospectra of an operator with those of its finite-difference and spectral discretizations.

One problem with discretizations is unavoidable: for each N there is an upper limit on the frequency of waves which are well resolved. So, whereas in the continuous case the reflection coefficient R_π is the same for all the eigenvalues, in the finite-difference model $|R_\pi|$ approaches 1 for the modes having wave number near the maximum on the grid. As a result, the high-frequency eigenvalues of the discretization are quite close to the imaginary axis, and it would be impossible to use these matrices to produce a time evolution plot such as Fig. 2, at least without some form of high-frequency filtering. The Chebyshev method performs well farther from the real axis but ultimately has the same shortcoming. Fortunately, in this case the pseudospectra are periodic in the imaginary direction, so it suffices to compute them at well-resolved frequencies only. The pseudospectra of L in Figs. 3–5 were computed in the strip $0 \leqslant \operatorname{Im} z \leqslant 1$ with Chebyshev discretizations based on $N \approx 50$.

6. Conclusion

Table 1 summarizes the information gained about the behavior of the system (6)–(8), as measured by $\|e^{tL}\|$, through pseudospectral analysis. An eigenvalue analysis would completely reveal only the first line of the table, dealing with the long-time trend of $\|e^{tL}\|$. The behavior over shorter time scales is not captured by the spectrum because L is not normal (Theorem 1). Indeed, in the most nonnormal case $\delta = 1$ the spectrum is empty, yet the pseudospectra are still meaningful and can be used to predict the behavior of the evolution operator (Theorem 2). Discretizations of the continuous problem exhibit similar amounts of nonnormality.

Eigenvalue analysis can mislead or fail for the same reasons in more complicated and physically interesting problems. One example arises in hydrodynamic stability, as mentioned in the Introduction. Others include magnetohydrodynamics [3], the stability of numerical methods for partial differential equations [17, 20], and the convergence of iterative methods for nonsymmetric linear systems of equations [12, 13]. We view the present paper as a case study to aid the development of methods for these and other applied problems.

Table 1
Summary of relationships between the pseudospectra and the behavior of the system studied in this paper

System behavior ($\|e^{tL}\|$)	(Pseudo)spectral information ($\|(\lambda I - L)^{-1}\|$)	
Asymptotic decay rate	Spectral abscissa	(21)
Recurrence of steps	Translation invariance	(19), Theorem 1
Height of steps	Condition of eigenmode basis	(25)
Slope of steps	Numerical abscissa	Theorem 1
Compact support ($\delta = 1$)	Exponential growth rate	Theorem 2

References

[1] J.S. Baggett, Exponential type versus spectral abscissa: the Hille and Phillips example, *Semigroup Forum*, submitted.

[2] L. Boberg and U. Brosa, Onset of turbulence in a pipe, *Z. Naturforsch.* **43a** (1988) 697–726.

[3] D. Borba et al., The pseudospectrum of the resistive magnetohydrodynamics operator: resolving the resistive Alfvén paradox, *Phys. Plasmas* **1** (1994) 3151–3160.

[4] K.M. Butler and B.F. Farrell, Three-dimensional optimal perturbations in viscous shear flow, *Phys. Fluids A* **4** (1992) 1637–1650.

[5] S. Cox and E. Zuazua, The rate at which energy decays in a string damped at one end, *Indiana Univ. Math. J.*, to appear.

[6] H. Dym and H.P. McKean, *Fourier Series and Integrals* (Academic Press, New York, 1972).

[7] B. Engquist and A. Majda, Absorbing boundary conditions for the numerical simulation of waves, *Math. Comput.* **31** (1977) 629–651.

[8] K.O. Friedrichs, Symmetric hyperbolic linear differential equations, *Commun. Pure Appl. Math.* **7** (1954) 345–392.

[9] T. Kato, *Perturbation Theory for Linear Operators* (Springer, Berlin, 2nd ed., 1976).

[10] A. Majda, Disappearing solutions for the dissipative wave equation, *Indiana Univ. Math. J.* **24** (1975) 1119–1133.

[11] J.B. Marion and S.T. Thornton, *Classical Dynamics of Particles & Systems* (Harcourt Brace Jovanovich, San Diego, 3rd ed., 1988).

[12] N.M. Nachtigal, S.C. Reddy and L.N. Trefethen, How fast are nonsymmetric matrix iterations?, *SIAM J. Matrix Anal. Applications* **13** (1992) 778–795.

[13] N.M. Nachtigal, L. Reichel and L.N. Trefethen, A hybrid GMRES algorithm for nonsymmetric linear systems, *SIAM J. Matrix Anal. Applications* **13** (1992) 796–825.

[14] A. Pazy, *Semigroups of Linear Operators and Applications to Partial Differential Equations* (Springer, Berlin, 1983).

[15] J. Prüss, On the spectrum of C_0 semigroups, *Trans. Amer. Math. Soc.* **284** (1984) 847–857.

[16] S.C. Reddy, P.J. Schmid and D.S. Henningson, Pseudospectra of the Orr–Sommerfeld operator, *SIAM J. Appl. Math.* **53** (1993) 15–47.

[17] S.C. Reddy and L.N. Trefethen, Stability of the method of lines, *Numer. Math.* **62** (1992) 235–267.

[18] S.C. Reddy and L.N. Trefethen, Pseudospectra of the convection-diffusion operator, *SIAM J. Appl. Math.* **54** (1994) 1634–1649.

[19] P. Rideau, Contrôle d'un assemblage de poutres flexibles par des capteurs actionneurs ponctules: étude du spectre du système, Thèse, Ecole Nat. Sup. des Mines de Paris, Sophia-Antipolis, France, 1985.

[20] L.N. Trefethen, Lax-stability vs. eigenvalue stability of spectral methods, in: K.W. Morton and M.J. Baines, Eds., *Numerical Methods for Fluid Dynamics III* (Clarendon Press, Oxford, 1988) 237–253.

[21] L.N. Trefethen, Pseudospectra of matrices, in: D.F. Griffiths and G.A. Watson, Eds., *Numerical Analysis* 1991 (Longman, New York, 1992) 234–266.

[22] L.N. Trefethen, A. Trefethen, S.C. Reddy and T.A. Driscoll, Hydrodynamic stability without eigenvalues, *Science* **261** (1993) 578–584.

[23] K. Veselić, On linear vibrational systems with one-dimensional damping, *Applicable Anal.* **29** (1988) 1–18.

[24] K. Veselić, On linear vibrational systems with one-dimensional damping II, *Int. Eqs. Oper. Theory* **13** (1990) 883–897.

[25] J. Zabczyk, A note on C_0-semigroups, *Bull Acad. Polon. Sci.* **23** (1975) 895–898.